# *Inkjet-printing and Performance Evaluation of UHF RFID Tag Antennas on Renewable Materials with Porous Surfaces*

Toni Björninen, Johanna Virkki, Juha Virtanen, Lauri Sydänheimo, Leena Ukkonen
Department of Electronics and Communications Engineering
Tampere University of Technology
Tampere, Finland
toni.bjorninen@tut.fi

Manos M. Tentzeris
The School of Electrical and Computer Engineering
Georgia Institute of Technology
Atlanta, GA, USA
etentze@ece.gatech.edu

***Abstract*—Material choices in electronic devices have a huge impact on the environment. The use of environmental-friendly processes and renewable materials is a growing trend. We present the inkjet-printing of antennas for passive UHF RFID tags on wood, paper, and cardboard. We printed the prototype antennas without surface treatments. We evaluated the performance of the fully assembled tags through wireless tag measurements. The fabricated tags achieved 6-to-9.5 meters read range under the European RFID transmission regulations.**

***Index Terms— Antenna modeling, Inkjet-printing, Renewable materials, RFID, Wireless tag measurements, WSN***

## I. INTRODUCTION

Internet of things (IoT) is a conceptual vision to connect everyday items and devices in order to create a ubiquitous computing world. Things are expected to become active participants in business, information, and social processes where they are enabled to interact and communicate among themselves, with humans, and with the environment. IoT has a great potential e.g. in home automation, intelligent transportation, and healthcare [1]-[2]. Radio-frequency identification (RFID), wireless sensor networks (WSN) and ambient power harvesting play a key role in the development toward IoT, where omnipresent antennas and electronics will be seamlessly and unobtrusively integrated with items all around us.

In the future, material choices in wireless devices will have a huge effect on the environment. This is why the use of renewable, environmental-friendly materials and additive manufacturing methods, such as inkjet-printing, is a growing trend. Great potential lies in the use of wood and paper as platforms for antennas used in radio-frequency identification (RFID) tags, wireless sensor networks (WSN) and ambient power harvesting [3]-[4]. Importantly, the capability to print antennas and electronics directly on various surfaces would remove the need for additional platforms, hence improving the integration and reducing the cost of raw materials. This is important for bringing novel smart products into mass production.integration and reducing the cost of raw materials. This is important for bringing novel smart products into mass production.

Renewable materials, such as wood, paper, and cardboard are typical materials especially in construction and packaging industry. Due to the porosity and high surface roughness, these materials are challenging platforms for inkjet-printing. The ink droplets are easily absorbed in the wood and paper, preventing the nanoscale metallization particles contained in the ink from forming a conductive layer. However, inkjet-printing of conductive patterns directly – without surface treatments – on these materials, is a major practical aspect, as it will provide savings in the process cost and time.

We present the antenna design for passive UHF RFID tags embedded in wood structures. Antennas were simulated and then inkjet-printed on wood, paper and cardboard, and the performance of the fully assembled tags was evaluated in terms of the maximum read range estimated based on wireless tag measurements.

## II. MODELING OF A TAG ANTENNA FOR WOOD VENEER

A full-wave electromagnetic solver, ANSYS HFSS v12, based on finite element method, was used in antenna modeling. In the simulation, the wood veneer (moisture content 12 %wt) was modeled with the dielectric properties $\varepsilon_r$=2.2 and tan$\delta$=0.1, which were estimated based on [5]-[6]. To achieve seamless integration and protection toward environmental stresses, the antenna was designed to be embedded in between two $1\times300\times300$ mm$^3$ pieces of wood veneer. This removes the need for additional structures. Based on the measurements of ink layer cross-sections and ink datasheet [7], the antenna conductor was modeled as a uniform layer with the thickness and conductivity of 5 μm and 25 MS/m, respectively.

During testing, we found that to achieve the maximal antenna performance, it was best to align the main radiating current of the antenna along the grain of the wood. This provided the most reliable print outcome. Because of the

This research was funded by Finnish Funding Agency for Technology and Innovation (TEKES), Academy of Finland, Centennial Foundation of Finnish Technology Industries, and Finnish Forest Foundation.

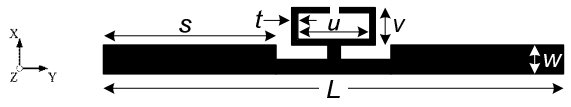


| Dimensional parameters in millimeters. | | | | | |
|---|---|---|---|---|---|
| *L* | *w* | *s* | *t* | *u* | *v* |
| 123.9 | 4 | 45.1 | 2.05 | 20 | 9.2 |

Figure 1. Tag antenna for wood veneer.

spreading of the ink, narrow traces and gaps in between adjacent traces were to be avoided. These application specific requirements were satisfied with a dipole antenna, which is a simple single-layer structure with well-known impedance matching and miniaturization techniques [8]-[9]. Compared with a slot-type antenna, which is another canonical single-layer antenna, dipole requires less ink and was hence considered a fit choice also from the cost perspective.

The prototype antenna is shown in Fig. 1. It is a straight dipole equipped with a T-matching loop (params. *u*,*v*,*t*). The loop transforms the capacitive impedance of the dipole to inductive. This makes it possible to achieve complex conjugate impedance matching between the antenna and the capacitive tag IC [8]. The additional coupling between the dipole body (params. *L*,*w*,*s*) and sections of the matching loop situated parallel to it allow for broadband matching, similar to what is achieved with the double T-matching technique [9]. We used the built-in genetic optimizer in the modeling tool to choose the matching loop parameters. The overall goal in the optimization was to achieve broadband and power-efficient impedance matching – in another words: to achieve high antenna realized gain over a broad range of frequencies.

Power reflection coefficient is the ratio of the power available from the tag antenna ($P_a$) and the power reflected back ($P_r$) from the antenna-chip interface due to impedance mismatch. It is related to antenna and IC impedances through

$$\Gamma = \frac{P_r}{P_a} = \left| \frac{Z_{ic} - Z_a^*}{Z_{ic} + Z_a} \right|^2, \qquad (1)$$

where $Z_a$ and $Z_{ic}$ are the antenna and IC impedances, respectively. Thus, the antenna realized gain is given by

$$G_r(\theta,\phi) = (1-\Gamma) D(\theta,\phi) e_r, \qquad (2)$$

where $D(\theta,\varphi)$ is the antenna directivity as a function of the spatial observation angle and $e_r$ is the antenna radiation efficiency. To evaluate equations (1-2) we used the simulated antenna properties and the tag IC impedance model based on [10]. All the associated parameters are shown in Fig. 2. Here the antenna gain is defined: $G(\theta,\varphi) = D(\theta,\varphi)e_r$. As a summary, our simulations predicted a fairly constant realized gain over the frequency range of 820-920 MHz. The simulated radiation efficiency remained also approximately constant: $0.60 \le e_r \le 0.66$. The broadside directivity was approximately 2 dBi, which is a typical value for a dipole antenna. Importantly, we achieved a broad 120 MHz (12%) matched bandwidth ($\Gamma \le 0.1$).

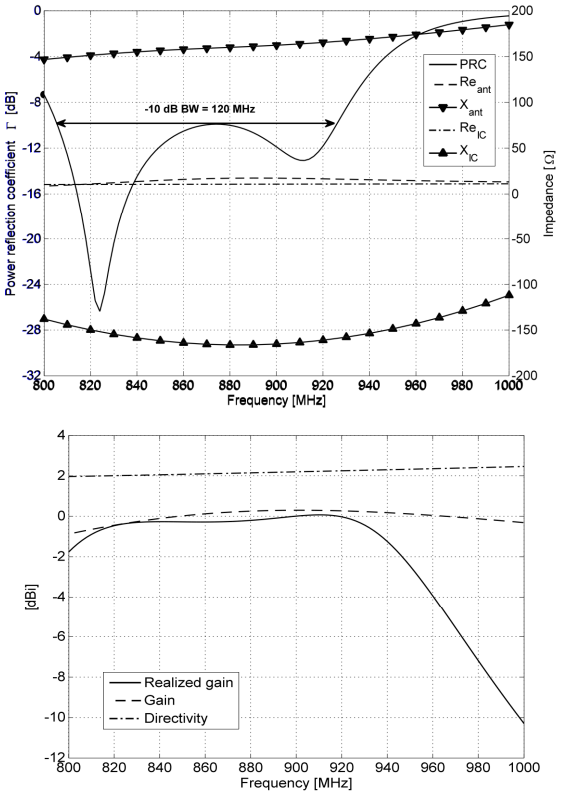


Figure. 2. Simulation results: antenna-IC impedance matching (top), radiation properties toward the positive z-axis shown in Fig. 1 (bottom).

## III. ANTENNA FABRICATION

### A. *Inkjet printing*

Inkjet printing is not just a single technique, but a collection of technologies aiming at the same target: forming small ink droplets and guiding them onto the substrate in a controlled way. In inkjet technology, small ink droplets (500 fl – 2nl) are formed in the printhead and ejected on the substrate. Inkjet printing allows the use of low viscosity inks, which is extremely important, since it allows for the formulation of inks that only contain an active material and solvents without the need for binders. In addition, inkjet allows cheap and contact-free manufacturing based on digital images. Although the digital images are readily swapped and modified, and no additional masks are required in the process, presently inkjet printing tends to be slow and high throughput is only achieved by using a large number of printheads in parallel. This has introduced yield concerns related to the misfiring of individual heads during printing of a pattern. Moreover, several process conditions must be accurately controlled for a successful print outcome. Most importantly, the ink droplets must have an appropriate shape and size when landing on the substrate. The drop form and velocity are controlled with the printhead parameters (distance to substrate, substrate temperature, jetting voltage and voltage waveform). These parameters need to be optimized for each ink and substrate.

Inkjet utilizes liquid materials, which sets some material requirements. The fluid should have certain viscosity (typically values between 8 and 25 Pa·s) and surface tension values (should remain between 2.8-3.3 N/m). Obviously, the requirements are also affected by the desired interaction with the chosen substrate. Currently, silver nanoparticles are commonly used as conductive fillers in inkjet ink formulations. In the future, copper and carbon based conductive inks may provide a more affordable alternatives [11]-[12].

### *B. Key parameters of the inkjet-printing process*

We fabricated the antennas on all the studied platforms with Fujifilm Dimatix DMP-2800 materials printer [13] using with 10 pl printhead nozzles and Harima NPS-JL silver nanoparticle ink [7]. The key parameters of the process are listed in Table 1. We considered NPS-JL especially suitable for creating conductive patterns on renewable materials, since it requires low sintering temperatures, 120 ˚C minimum. Using lower sintering temperatures will result in a slightly higher resistivity of the printed conductor, ranging between 4-6 μΩ·cm. This is approximately three times higher than the resistivity of bulk silver. In our work, we chose to use the temperature of 150 °C to maximize the conductivity of the ink layer [7].

TABLE I. KEY PARAMETERS OF THE INKJET-PRINTING PROCESS.

| Parameter | Value |
|---|---|
| Jetting voltage | 24 V |
| Jetting frequency | 9 kHz |
| Cartridge temperature | 40 ˚C |
| Platen temperature | 60 ˚C |
| Drop volume | 10 pl |
| Printing resolution | 423 dpi (60 μm drop spacing) |

### *C. Printing and curing of the tags*

The substrate materials used in this research were birch veneer, normal packaging cardboard, and silk surface art paper. During testing, we found that to achieve the maximal antenna performance on wood, it was best to align the main radiating current of the antenna along the grain of the wood. Thus, we aligned the dipole arms along the wood grain (Fig. 3b). Moreover, we found that to saturate the wood grain with ink, it was best to first print the five layers of ink with the printhead moving in the direction of the wood grain. After this, five more ink layers were added with the printhead moving against the wood grain. Following the ink datasheet instructions, we sintered the samples at 150 °C for 60 minutes to maximize the conductivity of the printed layer [7]. After sintering, we repeated the above described process a second time, to ensure sufficient conductor thickness for the antennas. Hence, we formed a conductor with total 20 ink layers with every five subsequent layers deposited with the printhead moving either along or against the grain of the wood.

Unlike the wood veneer, the paper and cardboard platforms did not have visible orientation dependent surface features. Thus, on these platforms, we printed the antennas with the printhead moving longitudinally along the dipole. To gain insight on the absorption of the ink into the cardboard, we printed the tags on this platform by using two different approaches. In the first approach, 20 layers of ink were deposited before sintering at 150 °C for 60 minutes. In the second approach, the same sintering conditions were used, but printing was done in two stages. First, 10 layers of ink were deposited before the first sintering, after which the process was repeated a second time. On the paper platform, we printed 15 layers of ink with the printhead moving longitudinally along the dipole followed by sintering at 150 °C for 60 minutes.

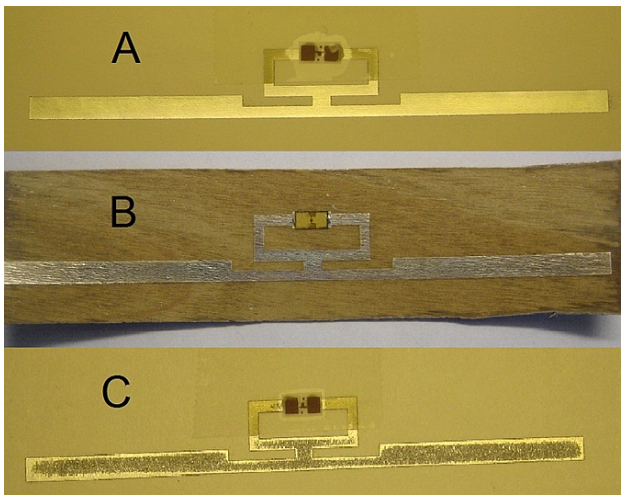


Figure 3. Inkjet-printed antennas with ICs on A) paper, B) wood, and C) cardboard.

After printing and curing, Alien Higgs-3 RFID ICs (tags printed on wood) and NXP RFID ICs (tags printed on paper and cardboard) were attached to the samples using a conductive silver epoxy resin. Both chips have the wake-up power of −18 dBm. Fig. 3 shows the fully assembled prototype tags.

TABLE II. KEY PARAMETERS OF THE INKJET-PRINTING PROCESS.

| **Substrate** | **Printing** | **Sintering** |
|---|---|---|
| Cardboard | 10 layers in the same direction, sintering (x2) | 150 ·C , 60 minutes |
| Cardboard | 20 layers in the same direction, sintering (x1) | 150 ·C , 60 minutes |
| Paper | 15 layers in the same direction, sintering (x1) | 150 ·C , 60 minutes |
| Wood | 5 layers in the direction of the grain, 5 layers against the grain, sintering (x2) | 150 ·C , 60 minutes |

## IV. TAG PERFORMANCE EVALUATION

We conducted wireless measurement on the prototype tags to evaluate their performance in terms of the theoretical read range. In the measurement, we used an RFID measurement system [14] which allowed us to monitor the reply from the tag under test to ISO-18006-C *query* command while sweeping the transmitted carrier power and the transmission frequency. Using the calibration tag included in the system hardware, we

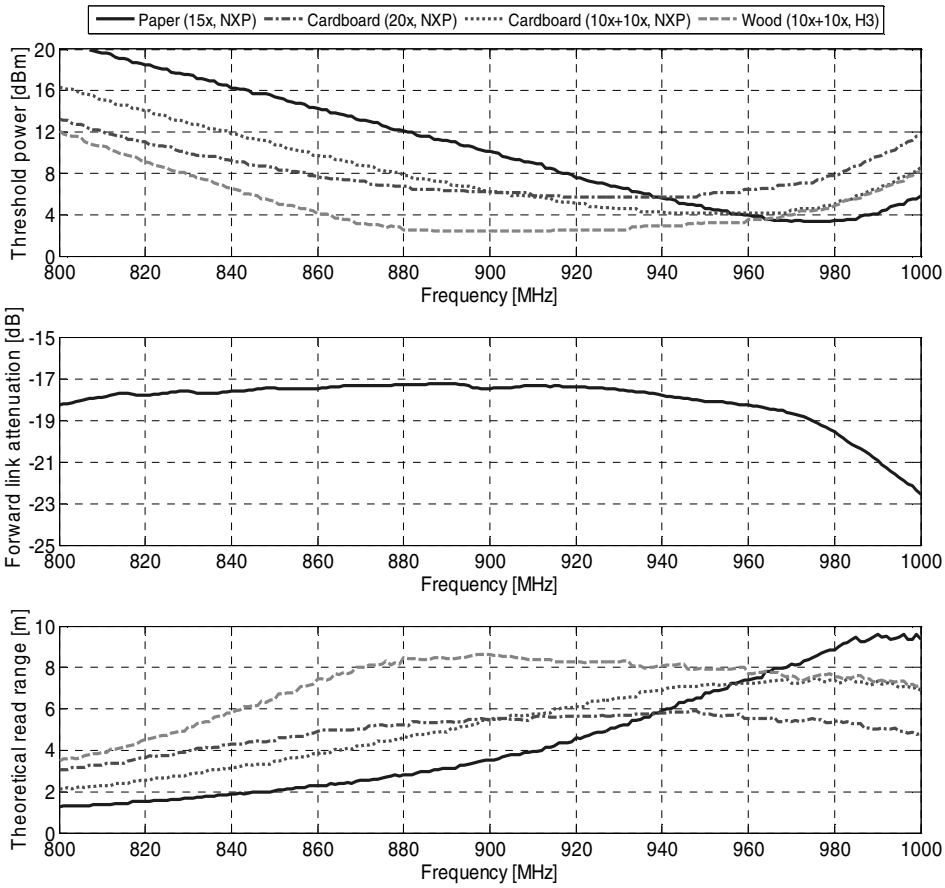


Figure 4. Measurement results.

also measured the path loss in the wireless measurement channel. The path loss is defined as the power loss factor ($L_{iso}$) from the transmitter's output port to the input port of a hypothetic polarization-matched isotropic antenna placed at the test location. To characterize the fabricated tags, we recorded the threshold power ($P_{th}$), the minimum reader output power which enabled a valid response from each tag. Based on the measured data, we computed theoretical read range from equation [9]

$$d_{tag} = \frac{\lambda}{4\pi}\sqrt{\frac{EIRP}{P_{th}L_{iso}}}, \qquad (3)$$

where *EIRP* is the regulated isotropically radiated power following the European regulation: *EIRP* = 3.28 W. In practice, the theoretical read range is attained in an anechoic environment in the main beam of a reader antenna which is polarization-matched with the tag antenna. Reporting the read range in these reference conditions provides a site-independent benchmark for researchers worldwide.

As seen from Fig. 4, the measured threshold power of the tag optimized for embedding in wood structures is the lowest around 900 MHz. This is the frequency where the fabricated tag attained its peak realized gain and the corresponding tag read range of 8.5 meters. Moreover, the threshold power remained fairly constant within the frequency range of 860-960 MHz with the corresponding tag read over seven meters. This confirmed the broadband response predicted by the simulations, but revealed a frequency shift of approximately 40 MHz toward higher frequencies. This is likely due to the fact that to facilitate the testing, we did not embed the fabricated antenna in between veneer layers as in the simulation.

The link attenuation is approximately the same for all tags, since the measurement channel was the same for all measured tags. The attenuation loss increased after 950 MHz due to the limited bandwidth of the transmit antenna.

We optimized the printed antenna for a tag embedded inside wood structures. However, we also fabricated the antenna on cardboard and paper for the purpose of further experimental performance evaluation. These additional tags were also equipped with a different tag IC. The chip has, however, similar impedance and the same wake-up power as the IC on the wood tag. Therefore, no major performance degradations were expected. As seen from Fig. 4, the paper tag actually achieved the highest read range (9.5 meters) among the studied tags. Beyond 970 MHz, the antenna printed on cardboard with sintering after 10 and 20 ink layers provided the same performance as the wood tag. Hence, we believe that with further platform- and IC-specific optimization it is possible to achieve equally good performance on cardboard and paper as well.

## V. CONCLUSION

Fabrication of antennas and electronics directly on renewable, environmental-friendly materials, such as wood and paper-based materials is imperative for the development of future wireless platforms. We presented passive UHF RFID tags with antennas inkjet-printed on wood, paper, and cardboard without any surface treatments. We provided guidelines for achieving reliable print outcome on the rough and porous surfaces. Our measurement results showed that the fabricated prototype tags on all the studied platforms achieved 6-to-8 meter read ranges under the European RFID transmission regulations. This performance is without a doubt sufficient for many future applications.

Future work will be the optimization the amount of the ink used as well as sintering times. We will also investigate the inkjet printing of copper inks as an alternative to silver inks for potential cost reduction.

## REFERENCES


[1] Commission of the European Communities, Internet of Things — An Action Plan for Europe, 2009. http://ec.europa.eu/information_society/policy/rfid/documents/commiot2009.pdf

[2] G. Kortuem, F. Kawsar, D. Fitton, V Sundramoorthy, "Smart objects as building blocks for the Internet of things," IEEE Internet Computing, vol. 14, no. 1, pp. 44-51, Jan.-Feb. 2010.

[3] G. Shaker, S. Safavi-Naeini, M. M. Tentzeris, "Inkjet printing of ultrawideband (UWB) antennas on paper-based substrates," IEEE Antennas Wireless Propag. Lett., vol. 10, no. 1., pp. 111-114, Dec. 2011.

[4] L. Yang, A. Rida, R. Vyas, M. M. Tentzeris "RFID tag and RF structures on a paper substrate using inkjet-printing technology," IEEE Trans. Microw. Theory Techn., vol. 55, no. 12, pp. 2894-2901, Dec. 2007.

[5] A. Koubaa, P. Perr, R. M. Hutcheon, J. Lessard, "Complex dielectric properties of the sapwoods of aspen, White Birch,Yellow Birch and Sugar Maple," Drying Technology, vol. 26, no. 5, pp. 568-578, May 1, 2008.

[6] M. Tabssum, B. Colpitts, K. Galik, "Dielectric Properties of Softwood Species Measured with an Open-ended Coaxial Probe," *8th Intl.IUFRO Wood Drying Conf.*, pp. 110-115, 24-29 Aug. 2003, Brasov, Romania.

[7] Harima Chemicals Group, Inc., Japan: http://www.harima.co.jp

NPS-JL nanopaste: http://www.harima.co.jp/en/products/pdf/16-17e.pdf

[8] G. Marrocco, "The art of UHF RFID antenna design: impedance-matching and size-reduction techniques," IEEE Antennas Propag. Mag. vol. 50, no. 1, pp. 66-79, Feb. 2008.

[9] T. Björninen, A. Z. Elsherbeni, L. Ukkonen, "Performance of single and double T-matched short dipole tag antennas for UHF RFID systems," J. Appl. Computational Electromagn. Soc., vol. 26, no. 12, pp. 953-962, Dec. 2011.

[10] T. Björninen, M. Lauri, L. Ukkonen, R. Ritala, A. Z. Elsherbeni, L. Sydänheimo, "Wireless measurement of RFID IC impedance," IEEE Trans. Instrum. Meas., vol. 60, no. 9, pp. 3194-3206, Sep. 2011.

[11] K. Woo, Y. Kim, B. Lee, J. Kim, J. Moon "Effect of carboxylic acid on sintering of inkjet-printed copper nanoparticulate films," ACS Appl. Mater. Interfaces, vol. 3, no. 7, pp. 2377-2382, May 2011.

[12] L. Huang, Y. Huang, J. Liang, X. Wan, Y. Chen, "Graphene-based conducting inks for direct inkjet printing of flexible conductive patterns and their applications in electric circuits and chemical sensors," Nano Research, vol. 4, no. 7, pp. 675-684, Jul. 2011.

[13] Fujifilm Dimatix, Inc., Santa Clara, CA, USA: http://www.fujifilmusa.com

[14] Voyantic, Ltd., Espoo, Finland: http://www.voyantic.com/